

DAF-16/FOXO targets genes that regulate tumor growth in *Caenorhabditis elegans*

Julie Pinkston-Gosse & Cynthia Kenyon

Cancer is an age-related disease, and inhibiting insulin/insulin-like growth factor 1 (IGF-1) signaling extends lifespan and increases tumor resistance in *C. elegans* and mammals. To investigate how the insulin/IGF-1 pathway couples these two processes, we analyzed putative transcriptional targets of the *C. elegans* FOXO transcription factor DAF-16, which promotes both longevity and tumor resistance. Twenty-nine of 734 genes tested influenced germline-tumor cell proliferation or p53-dependent apoptosis. About half of these genes also affected normal aging, thereby linking these two processes mechanistically. Many of these 29 genes are orthologs of known human tumor suppressors or oncogenes, suggesting that others may be as well. Our findings implicate nuclear-pore modification in p53-dependent cell death, because inhibiting nuclear-pore genes that are upregulated by DAF-16 blocks p53-dependent cell death in the tumor, but not normal, p53-independent, germline cell death.

In *C. elegans*, mutation of the *gld-1* tumor suppressor gene causes lethal germline tumors in which meiotic germ cells re-enter the mitotic cell cycle and proliferate extensively¹. In long-lived *daf-2* (insulin/IGF-1-receptor) mutants, *gld-1* tumors remain small and do not kill the animal². *daf-2* mutations counteract tumor growth by triggering germline apoptosis through the FOXO transcription factor DAF-16

and the tumor suppressor protein p53. In addition, *daf-2* mutations activate *daf-16*-dependent processes (and, to a lesser extent, *daf-16*-independent processes) that inhibit cell proliferation specifically within

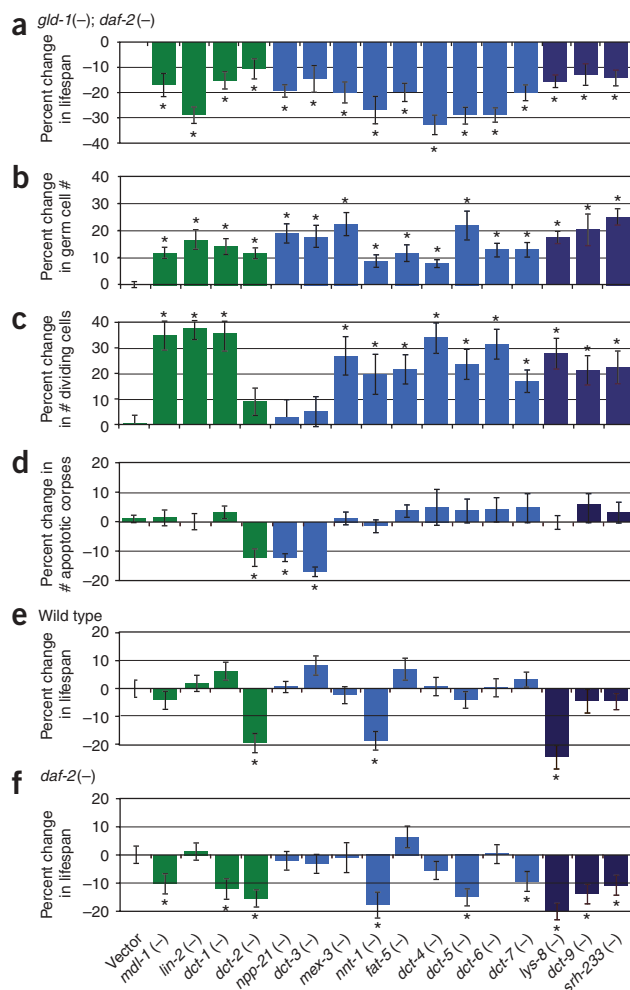


Figure 1 DAF-16/FOXO target genes that inhibit the growth of *gld-1* tumors. (a–c) Histograms show percent change in lifespan (a), approximate tumor size (b) and number (#) of actively dividing germ cells (c) of *gld-1(q485);daf-2(e1370)* animals subjected to RNAi of *gld-1*-tumor suppressor genes. Green, genes whose human orthologs are known tumor suppressor genes; blue, genes with orthologs in humans; dark blue, worm-specific genes. Approximate tumor size was determined using the DNA-intercalating dye DAPI, and number of actively dividing germ cells was scored using anti-phosphohistone H3 antibody staining, both of day-2 adults. (d) Histogram showing percent change in number of germ-cell corpses of *daf-2(e1370)* adults. Apoptosis was scored using the vital dye SYTO12. (e,f) Histogram showing percent change in the lifespans of wild-type (e) and *daf-2(e1370)* (f) animals treated with various RNAi clones. For statistical analysis see **Supplementary Tables 2–5** online; for individual lifespan curves, see **Supplementary Figure 4** online. Asterisks indicate $P \leq 0.01$. Error bars, s.e.m.

Department of Biochemistry and Biophysics, University of California San Francisco, San Francisco, California 94158, USA. Correspondence should be addressed to C.K. (ckenyon@biochem.ucsf.edu).

Received 8 June; accepted 14 August; published online 14 October 2007; doi:10.1038/ng.2007.1

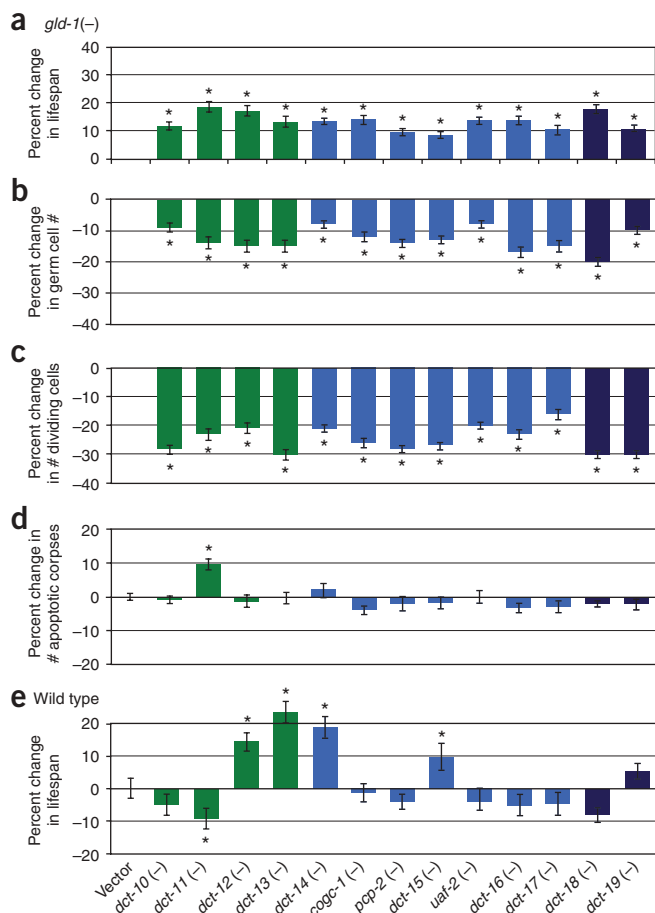


Figure 2 DAF-16/FOXO target genes that stimulate the growth of *gld-1* tumors. (a–c) Histograms show the percent change in lifespan (a), approximate tumor size (b) and number of actively dividing germ cells (c) of *gld-1(q485)* animals subjected to RNAi of *gld-1*-tumor stimulating genes. (d) Histogram showing percent change in number of germ-cell corpses of wild-type adults. (e) Histogram showing percent change in wild-type lifespans treated with various RNAi clones. Green, genes whose human orthologs are known oncogenes; blue, genes with orthologs in human; dark blue, worm-specific genes. For experimental detail, see legend for **Figure 1**. For statistical data, see **Supplementary Tables 2–5**; for lifespan curves, see **Supplementary Figure 5** online. Asterisks indicate $P \leq 0.01$. Error bars in a–e, s.e.m.

Sixteen of the 29 RNAi clones reduced lifespan and increased tumor cell number in *gld-1(-);daf-2(-)* animals by ~10–30% (**Fig. 1a,b**). Three of these *gld-1*-tumor suppressor genes were necessary for *daf-2* mutations to increase germ cell death within the tumor. One, *dct-2*, is homologous to mammalian GliPR1, which induces apoptosis in human prostate cancer cell lines via p53 (ref. 9).

The other two genes, *npp-21* and *dct-3*, both encode homologs of human Tpr, a component of the nuclear-pore complex (**Fig. 3**). Tpr appeared to affect tumor growth exclusively through apoptosis, because inactivation of *npp-21* had no effect on lifespan when apoptosis was prevented by a *ced-4(-)* mutation (**Fig. 3c**). Many proteins involved in apoptosis are transported through the nuclear pore¹⁰, and inhibiting nuclear-pore function has been shown to prevent apoptosis¹⁰. Consistent with this, RNAi knockdown or mutation of multiple nuclear pore-related genes (including the worm orthologs of nucleoporin-98 kDa and nucleoporin-214 kDa, which are disrupted in human leukemia¹¹) prevented apoptosis (**Fig. 3e,f** and **Supplementary Fig. 2** and **Supplementary Table 3** online), as did knockdown of the ortholog of the cargo-transport protein importin- α (**Fig. 3b**). We asked whether loss of apoptosis could be a trivial consequence of blocking DAF-16 from entering the nucleus, but *npp-21* inactivation affected neither DAF-16 nuclear localization nor the expression of a transcriptional target of DAF-16, *sod-3* (**Supplementary Fig. 2**).

In *C. elegans*, *daf-2* mutations and genotoxic stress both induce p53- and DAF-16-dependent cell death, whereas the apoptosis that takes place in the normal germline is largely DAF-16 and p53 independent^{2,12}. We found that *npp-21* RNAi completely prevented the cell death triggered by *daf-2* mutations and genotoxic stress but did not affect normal germ cell apoptosis (**Figs. 1d** and **3a,d**). It is possible that Tpr homologs are upregulated by DAF-16 in *daf-2* mutants (and presumably following DNA damage) to modify nuclear pores so that they can adequately transport a protein required specifically for p53-dependent cell death.

RNAi inactivation of the other 13 *gld-1*-tumor suppressor genes did not affect cell death but increased the number of mitotic germline-tumor cells in *gld-1(-);daf-2(-)* double mutants (**Fig. 1c**). Three of these genes are orthologs of known human tumor genes, encoding (i) the MAD family member Mxi1, which inhibits cell proliferation by antagonizing the Myc-Max interaction¹³; (ii) the protein kinase CASK, which also inhibits mammalian cell proliferation¹⁴; and (iii) the proapoptotic Bcl-2-interacting protein BNIP3, which may inhibit cell proliferation in addition to stimulating apoptosis¹⁵. Two of these cancer genes, those encoding Mxi1 and BNIP3, are known targets of mammalian FOXO3a^{4,16,17}.

The other mitotic *gld-1*-tumor suppressor genes have diverse functions (**Table 1**). One, *dct-5*, encodes a predicted zinc-finger

the tumor². Mutations that increase insulin/IGF-1 signaling or decrease FOXO activity promote tumor growth in mice and humans^{3,4}, suggesting that there may be conserved underlying mechanisms.

Because DAF-16/FOXO has a key role in tumor protection, we screened genes thought to be regulated by DAF-16 to investigate the underlying mechanism of *gld-1* tumor formation. To do this, we compiled a list of 734 direct or indirect DAF-16 target genes that had been identified previously using microarray analysis^{5,6} (S.-J. Lee and C.K., unpublished data), DAF-16 chromatin immunoprecipitation (ChIP)⁷ and comparative genomics⁸ (**Supplementary Table 1** online). As a primary screen, we used RNAi to identify genes that influence the lifespans of animals containing *gld-1* germline tumors. Next, we used 4,6-diamidino-2-phenylindole (DAPI) nuclear staining to identify genes affecting tumor cell number. To identify potential *gld-1*-tumor suppressor genes, we looked for RNAi clones that shortened lifespan and increased tumor size in long-lived *gld-1(-);daf-2(-)* double mutants; to identify potential *gld-1*-tumor stimulating genes, we looked for RNAi clones that extended lifespan and reduced the tumor size of short-lived *gld-1* single mutants. In all, we identified 29 genes that influenced tumor growth (**Figs. 1** and **2**). We confirmed that the expression of each gene was *daf-16* dependent using RT-PCR (**Supplementary Fig. 1** online), and, when available, we confirmed RNAi phenotypes using loss-of-function mutations (**Supplementary Table 2** online). All of these genes are listed in **Tables 1** and **2**, and the more informative ones are discussed below. We call the genes with previously unknown functions *dct* (DAF-16/FOXO-controlled tumor) genes.

Table 1 Genes that act downstream of DAF-16/FOXO to suppress *gld-1* tumors

Gene (<i>locus</i>)	Human ortholog	Description	Possible cell biological role	Consensus DAF-16 binding site within 5 kb of the promoter ^a
R03E9.1 (<i>mdl-1</i>)	MXI1 (MAX interactor 1 isoform b)	MAD family transcription factor	Inhibits cell growth by inhibiting Myc-Max interaction	1 canonical, 1 predicted
F17E5.1 (<i>lin-2</i>)	CASK (Ca ²⁺ /calmodulin-dependent serine protein kinase)	Membrane-associated kinase	Inhibits growth rate in ECV304 cells	1 canonical
C14F5.1 (<i>dct-1</i>)	BNIP3 (BCL2/adenovirus E1B 19-kDa-interacting 3)	BH3 domain	Promotes apoptosis; reduces proliferation index in tumors	3 predicted
ZK384.2 (<i>dct-2</i>)	GliPR 1 (glioma pathogenesis-related protein 1)	Defense-related, SCP domain	p53 target; promotes apoptosis	5 predicted
R07G3.3 (<i>npp-21</i>)	Nucleoprotein Tpr	Nuclear pore complex (NPC) protein	NPC components have been linked to cancer	1 canonical
C54D10.7 (<i>dct-3</i>)	Trichohyalin/nucleoprotein Tpr	Nuclear pore complex protein	NPC components have been linked to cancer	1 predicted
ZK384.1 (<i>dct-4</i>)	PI16 (protease inhibitor 16 precursor)	Defense-related, SCP domain	Signaling and innate immune response	2 predicted
C17G10.5 (<i>lys-8</i>)	None	Lysozyme activity, intestine rich	Innate immune response, TGF- β -like pathway	3 canonical
[C02A12.4 (<i>lys-7</i>)] ^c				
F53G12.5 (<i>mex-3</i>)	RKHD2 (ring finger/KH domain containing 2)	KH domain, RNA binding protein	GLD-1 target; loss of function causes transdifferentiation of <i>gld-1</i> cells into somatic cells	1 predicted
C15H9.1 (<i>nnt-1</i>)	NAD(P) transhydrogenase, mitochondrial precursor	Proton-pumping transhydrogenase	Electron transport chain activity	4 canonical, 1 predicted
W06D12.3 (<i>fat-5</i>)	Acyl-CoA desaturase	Fatty acid desaturase	Unsaturated fatty acid synthesis	1 canonical, 3 predicted
F07F6.5 (<i>dct-5</i>)	NFXL, <i>hozfp</i>	Zinc-finger transcription factor	Regulation of transcription	2 canonical
F25B5.1 (<i>dct-6</i>)	Isoform 4 of Golgin subfamily A member 4	Golgi autoantigen	Vesicular transport	2 canonical, 1 predicted
F15E6.8 (<i>dct-7</i>)	hnRNP A2 (heterogeneous nuclear ribonucleoprotein A2)	RNA-binding protein	RNA processing	2 canonical, 3 predicted
[F56D6.10] ^b (<i>dct-8</i>)				
W03F11.3 (<i>dct-9</i>)	None	PapD, major sperm protein domains	Unknown	1 canonical, 4 predicted
F47C12.3 (<i>srh-223</i>) ^e	None	Olfactory receptor	Some sensory mutations influence lifespan	1 canonical, 1 predicted
[F47C12.10 (<i>srh-222</i>)] ^d				

Genes whose human orthologs are known tumor genes in **boldface**.

^aCanonical: GTAAAC/TA or TTG/ATTAC; predicted: TGATAAG or CTTATCA. Each of these genes contained at least one consensus DAF-16 binding site within 5 kb of its promoter (compared to 78% using a random selection of genes²⁸). ^bWe expect that F15E6.8 (*dct-7*) will also hybridize to F56D6.10 (*dct-8*). ^cWe expect that C17G10.5 (*lys-8*) will also hybridize to C02A12.4 (*lys-7*). ^dWe expect that F47C12.3 (*srh-223*) will also hybridize to F47C12.10 (*srh-222*). ^e*srh-223* encodes a putative G-protein-coupled chemosensory receptor. Certain sensory neurons and chemoreceptors have been shown to have DAF-16-dependent effects on lifespan²⁹, so this could be a DAF-16 target gene that feedback-regulates the activity of the DAF-2 pathway. Consistent with this, reduction of *srh-223* blocked DAF-16 nuclear accumulation in *daf-2(-)* mutants (**Supplementary Fig. 2**) and shortened their lifespans (**Fig. 1f**).

the lifespans of normal animals that do not have tumors. Reducing the activity of six of the *gld-1*-tumor suppressor genes shortened the lifespans of *daf-2(-)* mutants significantly when compared with the lifespans of wild-type animals, suggesting that these genes promote longevity as well as tumor resistance (**Fig. 1e,f**). Among these, two were known human cancer genes, encoding the BH3-domain protein DCT-1/BNIP3 and the transcriptional regulator MDL-1/Mxi1 (*mdl-1* has previously been shown to promote longevity in *daf-2* mutants⁵), and one encoded the zinc finger transcription factor DCT-5.

RNAi inhibition of three genes, including the innate-immunity gene *lys-8*, shortened lifespan in both wild-type animals and *daf-2* mutants (**Fig. 1e,f**). *C. elegans* lives longer when it is fed bacteria that cannot divide²⁴, so inhibiting *lys-8* may increase the lifespan-shortening effects of bacteria. However, we cannot rule out the possibility that inactivation of any of these genes simply compromises the health of the animals.

Four of the *gld-1*-tumor stimulating genes also influenced lifespan; inhibiting these genes extended the lifespan of wild-type animals

(independently of *daf-16*, as predicted; **Supplementary Table 4** online) (**Fig. 2e**). Two of these are known human cancer genes, the adenosine A3 receptor gene *dct-12* and the putative transcription factor gene *dct-13*, predicted to encode an ortholog of Brfl1.

Finally, RNAi of *dct-11/LAPTM4B*, whose normal function promotes cell survival and proliferation, conferred tumor protection but shortened normal lifespan. Such a trade-off has been seen in mammals; for example, certain p53 mutations decrease tumor incidence but accelerate aging²⁵. Perhaps the deleterious effects of such mutations were counteracted during the evolution of longevity by the activity of the many genes that couple longevity to tumor resistance.

In summary, we have identified 29 DAF-16/FOXO-regulated genes that act in the insulin/IGF-1 pathway to influence *C. elegans* tumor growth. Some of these genes are required for the entire effect that *daf-2* mutations have on cell death, but none appear to be required for the entire effect on cell division. Because both increased apoptosis and reduced cell proliferation contribute to the tumor-protective effects of



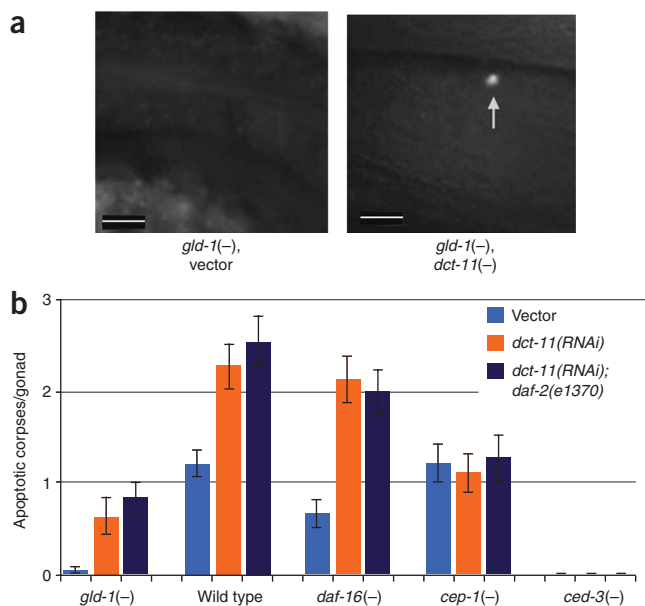


Figure 4 DCT-11 antagonizes the DNA-damage cell death pathway to inhibit germ cell death in *gld-1(-)* mutants. **(a)** RNAi inhibition of *dct-11* restores germ-cell death in *gld-1* mutants. **(b)** *cep-1* and *ced-3* mutations, but not *daf-16* mutations, block the increase in cell death by *dct-11* RNAi, in a wild-type and *daf-2* mutant background. These findings allow us to order these genes in a pathway, in which DAF-16 acts upstream of p53 through DCT-11. Error bars in **b**, s.e.m.

daf-2 mutations², together these downstream genes are likely to act in a cumulative fashion to influence tumor growth, much as downstream targets of DAF-16 appear to act cumulatively to influence lifespan⁵⁻⁸. In a limited test of this idea, we found that subjecting animals to RNAi of *mdl-1* and *npp-21* together produced a larger effect on tumor size

than did treatment with either *mdl-1* RNAi or *npp-21*RNAi alone (**Supplementary Fig. 3** online). Notably, almost half of the genes that affect tumor growth also affect the lifespans of animals that do not have tumors, indicating that the ability of the insulin/IGF-1 pathway to couple longevity and tumor resistance extends downstream of DAF-16.

The probability of finding a human tumor-related gene by chance in *C. elegans* is only ~1–2% (see Methods)²⁶. In contrast, 25% of the genes we identified were homologous to known human tumor suppressors or oncogenes, and others, such as those affecting innate immunity and the nuclear pore, affect processes that have been linked to cancer. This suggests that the biology of *gld-1* tumors has much in common with human tumor cell biology, and it raises the possibility that orthologs of some of these new genes will prove to be human oncogenes or tumor suppressors. Finally, because the screen was focused on the insulin/IGF-1/FOXO pathway in *C. elegans*, it will be valuable to learn whether the human orthologs of these genes are also regulated by insulin/IGF-1 signaling and FOXO.

Table 2 Genes that act downstream of DAF-16/FOXO to stimulate *gld-1* tumors

Gene (<i>locus</i>)	Human ortholog	Description	Possible cell biological role	Consensus DAF-16 binding site within 5 kb of the promoter ^a
Y38H6C.5 (<i>dct-10</i>)	PEG10 (imprinted paternally expressed 10)	Imprinted gene	Cell cycle, c-MYC target	2 canonical
W06B11.3 (<i>dct-11</i>)	LAPTM4B (lysosomal-associated protein transmembrane 4B)	Membrane transporter	Promotes cell survival and proliferation	2 canonical, 3 predicted
Y57A10C.7 (<i>dct-12</i>)	A3AR (adenosine A3 receptor)	G-protein-coupled receptor	Promote or inhibits cell growth	1 canonical
Y116A8C.17 (<i>dct-13</i>)	Brf1/Brf2 (butyrate response factor 1/2)	CCCH-type zinc-finger protein	Promotes myeloid cell proliferation	1 canonical
Y38H6C.3 (<i>dct-14</i>)	TSARG1 (testis/spermatogenesis cell apoptosis protein 1)	HSP40 protein family	Germ cell apoptosis	0
F23B2.12 (<i>pcp-2</i>)	Dipeptidyl-peptidase 2 precursor	Lysosomal serine protease	Cell growth and quiescence	4 canonical, 1 predicted
[F23B2.11 (<i>pcp-3</i>)] ^c				
W08D2.3 (<i>dct-15</i>)	Mfsd4 (major facilitator superfamily domain 4)	Plasma membrane transporter	Carbohydrate transport	1 canonical, 1 predicted
Y116A8C.35 (<i>uaf-2</i>)	U2AF35 (U2 snRNP splicing factor subunit)	Splicing factor	Mitotic progression (in HeLa cells)	2 canonical
Y38H6C.1 (<i>dct-16</i>)	Hypothetical	Similar to <i>Campylobacter jejuni</i> dnaK HSP70	Microbial infection	2 canonical
F35E12.7 (<i>dct-17</i>)	Intestinal mucin	Glycosylated protein	Aberrant expression in various malignancies	4 canonical, 2 predicted
Y54E10A.2 (<i>cogc-1</i>)	COG1 (component of oligomeric golgi complex 1)	Protein trafficking	<i>C. elegans</i> gonad morphogenesis	1 canonical
F58G1.4 (<i>dct-18</i>)	None	Uncharacterized	Unknown	3 canonical, 2 predicted
C32H11.13 (<i>dct-19</i>)	None	Uncharacterized	Unknown	2 canonical, 1 predicted

Genes whose human orthologs are known tumor genes are **boldface**.

^a93% of these genes contained at least one consensus DAF-16 binding site within 5 kb of its promoter (compared to 78% using a random selection of genes²⁸). Many of these genes also contained one or more DAF-16 binding sites within the coding region, including *dct-14*. ^bWe expect that *dct-13* will also hybridize to Y116A8C.20. ^cWe expect that F23B2.12 (*pcp-2*) will also hybridize to F23B2.11 (*pcp-3*).

METHODS

Strains. We used the following strains in this study: wild-type N2, *daf-2(e1370)*, *daf-16(mu86)*, *ced-3(n1286)*, *ced-4(n1162)*, *gld-1(q485)*, *cep-1(gk138)*, *ima-1(gk200)*, *abl-1(ok171)*, *npp-14(ok1389)*, *npp-11(ok1599)*, *cogc-1(k179)*, *nnt-1(ok794)*, *25B5.1(ok989)*, *hus-1(op241);unc-119(ed3);opIs34,daf-16(mu86);muIs109 [Pdaf-16::gfp::daf-16]* and *sod-3::GFP*.

RNAi screen for *gld-1*–tumor suppressors and promoters. To screen for *gld-1*–tumor suppressors, we tested genes shown by microarrays to be upregulated in *daf-2(-)* mutants in a *daf-16*-dependent fashion, as well as potential DAF-16 targets identified using ChIP and comparative genomic analysis. To identify potential *gld-1*–tumor stimulating genes, we tested genes that were downregulated in *daf-2* microarrays, along with genes identified using ChIP and comparative genomics.

RNAi was carried out by feeding. Each RNAi bacterial clone was inoculated in LB plus 10 µg/ml tetracycline and 100 µg/ml carbenicillin, grown overnight at 37 °C and seeded onto normal nematode growth medium–carbenicillin plates with 100 µl 0.1 M isopropyl-β-D-thiogalactoside (IPTG). Worms were fed RNAi bacteria from hatching. On day 1 of adulthood, ~50 *gld-1(q485);daf-2(e1370)* animals (or *gld-1(q485)* mutants for the *gld-1*–tumor promoter screen) were picked and transferred to a new RNAi plate. *gld-1* mutants are sterile, so the animals remained on the same plate for the remainder of the screen. We scored the viability of the worms on each plate approximately every other day from day 7 to day 13 of adulthood for *gld-1* single mutants, and day 20 to day 35 of adulthood for *gld-1(q485);daf-2(e1370)* double mutants. We then carried out full quantitative lifespan analysis for each bacterial strain that scored positive in the screen.

Following, we determined germ-cell estimates for each of the positive bacterial strains. Germ-cell estimates were determined blindly by counting 50 nuclei sections and multiplying by the number of total sections per gonad arm, and averages were calculated for ~50 animals per condition. Finally, to determine the change in germ-cell number, we compared these averages to those from vector-control animals. *P* values were determined using *t*-tests.

Analysis of RNAi clones. To verify the identity of each of the positive RNAi clones, we sequenced each insert using an M13-forward primer. Two of the genes identified in the screen, *cogc-1* and *uaf-2*, are located in operons. We tested whether genes that could be co-transcribed in these operons might have been knocked down by RNAi through ‘intra-operonic inhibition’. None of these RNAi clones produced similar phenotypes as those identified in the screen. Finally, possible secondary targets of each RNAi clone were determined using Wormbase RNAi Reports. For the RNAi clone *dct-12*, it was possible that Y57A10C.8 may have been knocked down. However, this RNAi clone did not produce the same phenotype as *dct-12* RNAi. Some of the RNAi clones were predicted to knock down two very closely related genes. These are indicated in **Supplementary Tables 2 and 5** online.

In addition, using RT-PCR, we confirmed that the expression of each gene identified in the screen is regulated by *daf-2* in a *daf-16* dependent fashion (**Supplementary Fig. 1**).

Lifespan analysis. For lifespan assays, we picked animals as L4 larvae at *t* = 0, and we transferred worms to new plates approximately every other day until the end of the reproductive period. Animals that were missing, or that died from extruded internal organs or from internally hatched progeny, were censored and statistically incorporated into the lifespan analyses²⁷. All lifespan experiments were performed at 20 °C. We generated lifespan curves using Statview 4.5 (SAS), and we determined *P* values using the Mantel-Cox log-rank test. Each lifespan experiment was repeated at least two times and, when available, RNAi experiments were repeated using mutants.

Fluorescence microscopy. For DAPI nuclear staining, gonads were dissected, fixed and stained with DAPI as described¹.

To visualize mitotic germ cells, we used anti-phosphohistone H3 antibody (Upstate Biotechnology) at a 1:400 dilution. Gonads were dissected and fixed with 3% formaldehyde for 20 min. For quantification of anti-phosphohistone H3–stained cells, we combined at least three separate experiments of ~20 animals to generate averages, and we determined *P* values using *t*-tests.

Apoptotic corpses were visualized using SYTO12 live imaging. We incubated animals in a 33 µM aqueous solution of SYTO12 for 4–5 h, and then we transferred them to seeded plates for 30 min before imaging. We determined averages by counting apoptotic corpses in ~20 animals in at least three separate experiments, and we determined *P* values using *t*-tests. For genotoxic-stress assays, apoptosis was scored 18 h after irradiation.

All images were captured using a Zeiss Axioplan, and images were rotated using Adobe Photoshop 7.0.

Probability of randomly finding a human cancer gene in worms. We first took a random set of 200 *C. elegans* genes using the ‘random gene selection’ program from Regulatory Sequence Analysis Tools (RSAT, <http://rsat.ulb.ac.be/rsat/>), and then we used WormBase to determine predicted human homologs for each gene. Using PubMed and OMIM, we then carried out a thorough search for possible roles of each gene in cancer. Using this criterion, we determined that four of these genes (2%) encoded predicted human cancer genes.

Quantitative RT-PCR. Real-time RT-PCR was carried out using the 7300 Real Time PCR System (Applied Biosystems, Foster City, CA, USA). Primers and probes were designed specifically for each gene using Primer3 software.

Note: Supplementary information is available on the Nature Genetics website.

ACKNOWLEDGMENTS

We thank S. Henis-Korenblit, M. Hansen and N. Gosse for careful reading of the text, and the Caenorhabditis Genetics Center and the *C. elegans* Gene Knockout Consortium for providing strains. This work was supported by US National Institutes of Health funding to C.K. J.P.-G. was supported by University of California San Francisco’s Chancellor’s fellowship. C.K. is an American Cancer Society Research Professor and a founder and director of Elixir Pharmaceuticals.

AUTHOR CONTRIBUTIONS

J.P.-G. carried out all the experiments. C.K. helped to design the experiments and write the paper.

Published online at <http://www.nature.com/naturegenetics>

Reprints and permissions information is available online at <http://npg.nature.com/reprintsandpermissions>

- Francis, R., Barton, M.K., Kimble, J. & Schedl, T. *gld-1*, a tumor suppressor gene required for oocyte development in *Caenorhabditis elegans*. *Genetics* **139**, 579–606 (1995).
- Pinkston, J.M., Garigan, D., Hansen, M. & Kenyon, C. Mutations that increase the life span of *C. elegans* inhibit tumor growth. *Science* **313**, 971–975 (2006).
- Ramsey, M.M. *et al.* Growth hormone-deficient dwarf animals are resistant to dimethylbenzanthracene (DMBA)-induced mammary carcinogenesis. *Endocrinology* **143**, 4139–4142 (2002).
- Paik, J.H. *et al.* FoxOs are lineage-restricted redundant tumor suppressors and regulate endothelial cell homeostasis. *Cell* **128**, 309–323 (2007).
- Murphy, C.T. *et al.* Genes that act downstream of DAF-16 to influence the lifespan of *Caenorhabditis elegans*. *Nature* **424**, 277–283 (2003).
- McElwee, J., Bubbs, K. & Thomas, J.H. Transcriptional outputs of the *Caenorhabditis elegans* forkhead protein DAF-16. *Aging Cell* **2**, 111–121 (2003).
- Oh, S.W. *et al.* Identification of direct DAF-16 targets controlling longevity, metabolism and diapause by chromatin immunoprecipitation. *Nat. Genet.* **38**, 251–257 (2006).
- Lee, S.S., Kennedy, S., Tolonen, A.C. & Ruvkun, G. DAF-16 target genes that control *C. elegans* life-span and metabolism. *Science* **300**, 644–647 (2003).
- Ren, C. *et al.* RTVP-1, a tumor suppressor inactivated by methylation in prostate cancer. *Cancer Res.* **64**, 969–976 (2004).
- Fahrenkrog, B. The nuclear pore complex, nuclear transport, and apoptosis. *Can. J. Physiol. Pharmacol.* **84**, 279–286 (2006).
- Kasper, L.H. *et al.* CREB binding protein interacts with nucleoporin-specific FG repeats that activate transcription and mediate NUP98-HOXA9 oncogenicity. *Mol. Cell. Biol.* **19**, 764–776 (1999).
- Schumacher, B., Hofmann, K., Boulton, S. & Gartner, A. The *C. elegans* homolog of the p53 tumor suppressor is required for DNA damage-induced apoptosis. *Curr. Biol.* **11**, 1722–1727 (2001).
- Wechsler, D.S., Shelly, C.A., Petroff, C.A. & Dang, C.V. *MXI1*, a putative tumor suppressor gene, suppresses growth of human glioblastoma cells. *Cancer Res.* **57**, 4905–4912 (1997).
- Qi, J. *et al.* CASK inhibits ECV304 cell growth and interacts with Id1. *Biochem. Biophys. Res. Commun.* **328**, 517–521 (2005).
- Milner, A.E., Grand, R.J., Vaughan, A.T., Armitage, R.J. & Gregory, C.D. Differential effects of BCL-2 on survival and proliferation of human B-lymphoma cells following gamma-irradiation. *Oncogene* **15**, 1815–1822 (1997).

16. Delpuech, O. *et al.* Induction of Mxi1-SR(alpha) by FOXO3a contributes to repression of Myc-dependent gene expression. *Mol Cell Biol* (2007).
17. Modur, V., Nagarajan, R., Evers, B.M. & Milbrandt, J. FOXO proteins regulate tumor necrosis factor-related apoptosis inducing ligand expression. Implications for PTEN mutation in prostate cancer. *J. Biol. Chem.* **277**, 47928–47937 (2002).
18. Zhou, L. *et al.* Overexpression of LAPT4B–35 closely correlated with clinicopathological features and post-resectional survival of gallbladder carcinoma. *Eur. J. Cancer* **43**, 809–815 (2007).
19. Li, C.M. *et al.* PEG10 is a c-MYC target gene in cancer cells. *Cancer Res.* **66**, 665–672 (2006).
20. Madi, L. *et al.* The A3 adenosine receptor is highly expressed in tumor versus normal cells: potential target for tumor growth inhibition. *Clin. Cancer Res.* **10**, 4472–4479 (2004).
21. Ohana, G., Bar-Yehuda, S., Barer, F. & Fishman, P. Differential effect of adenosine on tumor and normal cell growth: focus on the A3 adenosine receptor. *J. Cell. Physiol.* **186**, 19–23 (2001).
22. Shimada, H. *et al.* Analysis of genes under the downstream control of the t(8;21) fusion protein AML1-MTG8: overexpression of the TIS11b (ERF-1, cMG1) gene induces myeloid cell proliferation in response to G-CSF. *Blood* **96**, 655–663 (2000).
23. Singh, A.P., Chaturvedi, P. & Batra, S.K. Emerging roles of MUC4 in cancer: a novel target for diagnosis and therapy. *Cancer Res.* **67**, 433–436 (2007).
24. Garigan, D. *et al.* Genetic analysis of tissue aging in *Caenorhabditis elegans*: a role for heat-shock factor and bacterial proliferation. *Genetics* **161**, 1101–1112 (2002).
25. Tyner, S.D. *et al.* p53 mutant mice that display early ageing-associated phenotypes. *Nature* **415**, 45–53 (2002).
26. Futreal, P.A. *et al.* A census of human cancer genes. *Nat. Rev. Cancer* **4**, 177–183 (2004).
27. Lawless, J.F. *Models and Methods for Lifetime Data* (Wiley, New York, 1998).
28. Kenyon, C. & Murphy, C.T. Enrichment of regulatory motifs upstream of predicted DAF-16 targets. *Nat Genet* **38**, 397–8 ; author reply 398 (2006).
29. Alcedo, J. & Kenyon, C. Regulation of *C. elegans* longevity by specific gustatory and olfactory neurons. *Neuron* **41**, 45–55 (2004).
30. Nakielnny, S. & Dreyfuss, G. Transport of proteins and RNAs in and out of the nucleus. *Cell* **99**, 677–690 (1999).